

# Infra-red Spectroscopic Studies of $\text{GdBaCo}_2\text{O}_{5.5}$

Shraddha Ganorkar, K. R. Priolkar \*

*Department of Physics, Goa University, Goa, 403 206 India.*

---

## Abstract

This paper reports infrared spectroscopic studies on  $\text{GdBaCo}_2\text{O}_{5.5}$  layered perovskite which exhibits successive magnetic transitions from paramagnetic to ferromagnetic to antiferromagnetic states as well as high temperature metal to insulator transition and a change in charge transport mechanism at low temperature. Infrared absorption spectra recorded at various temperatures in the range 80 K to 350 K reveal changes in the positions of Co-O stretching and bending frequencies which provide an explanation to the magnetic and transport behaviour of this compound.

*Key words:*  $\text{GdBaCo}_2\text{O}_{5.5}$ , Layered Perovskites, Infrared absorption

*PACS:* 72.10.Di; 78.30.-j; 87.64.Je

---

## 1 Introduction

The study of transition-metal oxides has become a very attractive field during the last years. They exhibit a complex interplay between charge, spin, and lattice degrees of freedom which is the heart of many fascinating phenomena like Colossal Magnetoresistance (CMR), superconductivity etc. Among them, cobalt oxides are subject of vivid studies because cobalt shows great facilities to present different spins states at different temperatures.

The spin-state degree of freedom of Co ions introduces new effects in these narrow band oxides[1]. The existence of several possible spin states in given oxidation state makes cobaltites a rich but challenging system to study.  $\text{Co}^{3+}$  has three possible spin states: the low spin state (LS,  $t_{2g}^6 e_g^0$ ,  $S=0$ ), the intermediate spin state (IS,  $t_{2g}^5 e_g^1$ ,  $S=1$ ) and high spin state (HS,  $t_{2g}^4 e_g^2$ ,  $S=2$ ) which

---

\* Corresponding author

*Email address:* [krp@unigoa.ac.in](mailto:krp@unigoa.ac.in) (K. R. Priolkar).

arise from the competition between crystal field, on-site Coulomb correlation and the inter atomic exchange energy [2].

The  $\text{RBaCo}_2\text{O}_{5.5}$  ( $\text{R} = \text{rare earth}$ ), in particular, displays a variety of interesting phenomena including metal insulator transition [3,4], spin state transition [5,6], charge ordering [7,8] and giant magnetoresistance [8,9]. The crystal structure consists of sandwiches  $\text{CoO}_2 - \text{BaO} - \text{RO}_{0.5} - \text{CoO}_2$  stacked along c-axis of orthorhombic lattice. The doubling of b-axis originates from an alternation of  $\text{CoO}_5$  square pyramids and  $\text{CoO}_6$  octahedra along this direction. In contrast to  $\text{RCoO}_3$  [14,15,16,17], the octahedra and pyramids are heavily distorted [10,11]. This distortion supports a variety of  $\text{Co}^{3+}$  spin state [LS, IS and HS] [12,13] as a function of crystallographic environment and temperature.

A metal-insulator transition (MIT) is present in several  $\text{RBaCo}_2\text{O}_{5.5}$  compounds [4]. An anomalous change of lattice parameters have been reported at the MIT temperature for  $\text{GaBaCo}_2\text{O}_{5.5}$  and  $\text{TbBaCo}_2\text{O}_{5.5}$  implying that the transition is related to changes in structure [5,18]. While magnetic susceptibility measurements indicate the MIT to be associated with spin state transition of  $\text{Co}^{3+}$  ion [2,5,19]. It has been proposed that the insulating state below MIT temperature is promoted by the ordering of cobalt spin states with LS and IS states respectively in octahedrally and pyramidally coordinated sites [3]. Further, using neutron diffraction studies it is suggested that, octahedrally coordinated Co ions undergo a spin state transition from HS to IS or LS state in the insulating phase, while pyramidally coordinated Co ions remain in the IS state [5,2]. Another scenario that has been put forth based on electron diffraction and microscopy studies is the coexistence of IS (pyramids) and LS (octahedra) for  $T < T_{MI}$  ( $T_{MI}$  - metal to insulator transition temperature) and HS  $\text{Co}^{3+}$  at higher temperatures [4]. Therefore, the spin state of Co ions on both sides of the MIT is still not clear.

Furthermore, several magnetic transitions have been reported for these compounds. Just below  $T_{MI}$  the compounds undergo a paramagnetic (PM) to ferro(ferri)magnetic (FM) transition followed by a FM to antiferromagnetic (AFM1) transition which is accompanied by an onset of strong anisotropic magneto-resistive effects and AFM1 to second antiferromagnetic (AMF2) phase transition. The mechanism of such magnetic transformations at low temperature is still to be properly understood. It is also not clear why subtle changes in oxygen content should cause drastic changes in magnetic properties [20,21]. Various contradicting magnetic structure including different spin state of  $\text{Co}^{3+}$  ions and also spin state ordering (SSO) have been proposed, based on neutron diffraction [22,23,24,25] and macroscopic measurements [26]. Muon-spin relaxation ( $\mu\text{SR}$ ) studies reveal that irrespective of the rare earth ion, a homogeneous FM phase with ferrimagnetic SSO of IS and HS states develops through two first order phase transitions into phase separated AFM1 and AFM2 phases with different types of antiferromagnetic SSO [27]. Density functional calcu-

lations suggest that there is a strong hybridization between O-2p and Co-3d orbitals with a narrow charge transfer gap near Fermi level, which gives rise to  $pd\sigma$  hybridized hole in the O-2p valence band. With increasing temperature, a gradual delocalization of the  $pd\sigma$  holes in the almost HS  $\text{Co}^{3+}$  is responsible for the successive magnetic transitions accompanied by spin reorientation in a spin-canted structure due to competing FM and AFM interactions [12,28]. Resonant photoemission studies also support this picture [29].

## 2 Experimental

The polycrystalline sample of  $\text{GdBaCo}_2\text{O}_{5.5}$  was prepared using conventional solid-state reaction method.  $\text{Gd}_2\text{O}_3$  and  $\text{BaCO}_3$  were preheated at  $900^\circ\text{C}$  and  $700^\circ\text{C}$  respectively for 12 hours. Stoichiometric amount of  $\text{Gd}_2\text{O}_3$ ,  $\text{BaCO}_3$  and  $\text{Co}(\text{NO}_3)_3 \cdot 6\text{H}_2\text{O}$  were dissolved in  $\text{HNO}_3$ . This mixture was stirred continuously using a magnetic stirrer for about 30 minutes to ensure proper mixing. The solution was allowed to settle for an hour and dried on a heater. This dried powder was then sintered in a furnace at  $1000^\circ\text{C}$  for 12 hours twice with an intermediate grinding to ensure homogeneity. Finally the sintered powder was ground again and pressed into pellets and annealed in oxygen atmosphere at  $1050^\circ\text{C}$  for 24 hours. The sample was furnace cooled at a rate of  $1^\circ\text{C}$  per minute. The sample was deemed to be phase pure, as X-ray diffraction (XRD) data collected on a Rigaku D-Max IIC X-ray diffractometer in the range of  $20^\circ \leq 2\theta \leq 80^\circ$  using  $\text{CuK}\alpha$  radiation showed no impurity reflections. The diffraction pattern was Rietveld refined using FULLPROF suite and structural parameters were obtained. The oxygen content verified by iodometric titration, was found to be  $\delta=5.5$ . The magnetization measurements were carried out as a function of temperature and magnetic field using a Quantum Design SQUID magnetometer at fields of 1000 Oe, in the temperature range of 5 K to 300 K. The magnetization measurements were carried out in both the zero-field cooled (ZFC) and field-cooled modes(FC). The temperature (100 K to 300 K) dependence of the electrical resistivity was measured using a standard four probe set up and a Keithley 2182 nanovoltmeter and Keithley constant current source. IR spectra were recorded on FTIR-8900 Shimadzu spectrophotometer with Oxford OPTIDNVA Cryostat with KRS5 windows in the temperature range 80 K to 350 K. These KRS5 windows give a sharp peak like feature around  $675\text{ cm}^{-1}$ .

### 3 Results and Discussion

XRD pattern presented in Fig. 1 shows the formation of a single phase sample. Rietveld refinement of the XRD pattern indicates that structure is orthorhombic with Pmmm space group. The lattice parameters obtained from fitting are  $a = 3.8760(4)\text{\AA}$ ,  $b = 7.822(1)\text{\AA}$  and  $c = 7.533(1)\text{\AA}$  which agree well with those reported in literature for  $\text{GdBaCo}_2\text{O}_{5.45}$  [19]. Iodometric titration reveals the value of  $\delta = 0.5$ .

The temperature dependence of magnetization  $M(T)$  is shown in Fig.2. Upon cooling  $M(T)$  in both ZFC and FC cycles increases rapidly indicative of a PM to FM transition at  $T_c = 275$  K. It reaches a maximum at around 250 K and starts decreasing with further lowering of temperature. Around  $T \simeq 230$  K and  $T = 210$  K there are appearances of two magnetic transitions which are reported to be AFM. At still lower temperatures ( $T \leq 100$  K) the magnetization shows paramagnetic behaviour which is attributed to Curie-Weiss behaviour of Gd sub-lattice [19].

The resistivity as a function of temperature is plotted in Fig.3(a). At 350 K there is a clear signature of MI transition followed by a broad hump which coincides with PM - FM transition. Further, one more anomaly is seen at 164 K which has been attributed to strong coupling between the spin order and charge carriers [30]. Below  $T < 164$  K resistivity follows Mott's variable range hopping (VRH) model as can be clearly seen in Fig 3(b).

Fourier transform infrared (IR) absorption spectra at various temperatures in the range  $350 \text{ K} \leq T \leq 80 \text{ K}$  are presented in Fig.4. The optical phonon bands appear in the range  $500 \text{ cm}^{-1}$  to  $600 \text{ cm}^{-1}$ .  $\text{RBaCo}_2\text{O}_{5.5}$  compounds being derivatives of  $\text{RCoO}_3$  single perovskites, the same nomenclature can be used to classify the absorption modes. As per the nomenclature available for  $\text{RCoO}_3$  compounds, there are eight IR active modes reported for  $\text{RCoO}_3$  system of which the modes around  $600 \text{ cm}^{-1}$  are called stretching modes and those around  $500 \text{ cm}^{-1}$  are termed as bending modes. The stretching modes can be fitted with three Gaussian's and one Lorentzian [31].

In  $\text{RCoO}_3$ ,  $\text{Co}^{3+}$  is in LS state at low temperatures. With increase in temperature, the crystal-field splitting decreases and two excited states (IS and HS) can be populated [33,34]. Since these spin states are very close in energy, transitions to these higher spin state can occur either with variation in temperature or with deformation of the crystal lattice. The frequencies of IR vibration modes exhibit anomalies at these spin state transition temperatures. Generally the vibration modes harden when the sample undergoes a transition from IS/HS to LS state. If the magnetic transitions observed in  $\text{GdBaCo}_2\text{O}_{5.5}$  are due to spin state transformation then its lattice vibration modes should

also show similar temperature dependence.

In order to examine the temperature dependence of frequencies of Co-O stretching and bending modes in  $\text{GdBaCo}_2\text{O}_{5.5}$ , the IR absorption spectra from 500 to  $650\text{ cm}^{-1}$  were fitted with Gaussian peaks. At 350 K the IR spectra can be fitted with four Gaussians, bending modes centred at 503,  $535\text{ cm}^{-1}$  and stretching modes at 560 and  $587\text{ cm}^{-1}$ . At lower temperature a new stretching mode appears at  $626\text{ cm}^{-1}$  due to anomalous cell contraction as a consequence of the metal to insulator transition [25]. The observed absorption modes are in agreement with the IR absorption bands reported for  $\text{TbBaCo}_2\text{O}_{5.5}$  [32]. The spectra at 300 K and lower temperatures can be best fitted with five Gaussian peaks at 510, 534, 571, 600 and  $626\text{ cm}^{-1}$ . The fitting to the experimental data is shown as continuous line in Fig. 4. The temperature evolution of the IR stretching frequencies is plotted in Fig.5. The bending mode at  $503\text{ cm}^{-1}$  shifts continuously toward higher wavenumber from 350K to 150 K and then shows a decrease in its frequency below 150 K. The second bending mode at  $534\text{ cm}^{-1}$  has nearly temperature independent evolution down to 150K, below which it shifts towards lower frequencies and tends to merge with the other bending mode. The stretching modes 560, 588 and  $626\text{ cm}^{-1}$  at 350 K show a gradual increase in wavenumber. At 150 K the stretching modes show shift towards lower wavenumber, while at 80 K these modes harden again.

At 350 K the compound is a PM metal with  $\text{Co}^{3+}$  in HS state. As temperature decreases it undergoes a MI transition followed by PM to FM transition. These transitions are believed to be due to a change in  $\text{Co}^{3+}$  spin state from HS to IS concomitant with decrease in cell volume. These changes are reflected in IR absorption spectra by an increase in vibration frequency of 560 and  $588\text{ cm}^{-1}$  stretching modes by  $12\text{ cm}^{-1}$  and occurrence of a new mode at  $626\text{ cm}^{-1}$ . Very similar results have been reported in case of  $\text{RCoO}_3$  compound where it is observed that the IR vibration modes harden with decrease in temperature [31,35,36].

It can be seen that the stretching modes ( $560, 588$  and  $626\text{ cm}^{-1}$ ) shift towards lower wavenumber below 200 K which coincides with the appearance of AFM order and change in resistivity behaviour respectively. This softening of mode could be related to a larger deformation of Co-O polyhedra resulting in displacement of Co ions away from the ideal middle plane. This results in higher bending of Co-O-Co bonds. Reduction in Co-O-Co bond angle localizes the p-d holes favouring antiferromagnetic order. Such a change in Co  $3d$  and O  $2p$  hybridization has been predicted by density functional theory calculations as well observed in resonant photoemission studies [12,28,29]. The reduction of Co-O-Co bond angle will reduce the electron transfer integral through Co-O-Co network leading to higher resistivity. Indeed as can be seen from Fig. 3, resistivity below 164 K rises steeply and it follows the Mott's VRH law.

## 4 Conclusion

In conclusion, IR spectra of  $\text{GdBaCo}_2\text{O}_{5.5}$  shows changes in positions and intensities of Co-O stretching and bending which can be related to various magnetic transitions. Upon MI followed by PM to FM transition a stretching mode at appears at  $626\text{ cm}^{-1}$  due to  $\text{Co}^{3+}$  HS  $\rightarrow$  IS spin state transition and a decrease in cell volume. Further, IR absorption studies indicate that AFM transition is due to increase in p-d hybridization. This increase of p-d hybridization can also explain the change in resistivity behaviour at low temperatures.

## References

- [1] M. Rodríguez Carvajal and J. Goodenough, *J. Solid State Chem.* **116** 224 (1995).
- [2] C. Frontera, J. García-Muñoz, A. Llobet, and M. Aranda, *Phys. Rev. B* **65**, 180405 (2002).
- [3] C. Martin, A. Maignan, D. Pelloquin, N. Nguyen, and B. Raveau, *Appl. Phys. Lett.* **71**, 1421 (1997).
- [4] A. Maignan, C. Martin, D. Pelloquin, N. Nguyen, and B. Raveau, *J. Solid State Chem.* **142** 247 (1999).
- [5] Y. Moritomo, T. Akimoto, M. Takeo, A. Machida, E. Nishibori, M. Takata, M. Sakata, K. Ohoyama and A. Nakamura, *Phys. Rev. B* **61**, R13325 (2000).
- [6] M. Respaud, C. Frontera, J. García-Muñoz, M. Angel G., Aranda, B. Raquet, J. Broto, H. Rakoto, M. Goiran, A. Llobet, and J. Carvajal, *Phys. Rev. B* **64**, 214401 (2001).
- [7] T. Vogt, P. M. Woodward, P. Karen, B. A. Hunter, P. Henning, and A. R. Moodenbaugh, *Phys. Rev. Lett* **84**, 2969 (2000).
- [8] E. Suard, F. Fauth, V. Caignaert, I. Mirebeau and G. Baldinozziet, *Phys. Rev. B* **61**, R11871 (2000).
- [9] I. Troyanchuk, N. Kasper, and D. Khalyavin, *Phys. Rev. Lett* **80**, 3380 (1998).
- [10] D. Khalyavin, S. Barilo, S. Shiryayev, G. Bychkov, I. Troyanchuk, A. Furrer, P. Allenspach, S. Szymczak and R. Szymczak, *Phys. Rev. B* **67**, 214421 (2003).
- [11] E. Pomjakushina, K. Conder and V. Pomjakushin, *Phys. Rev. B* **73**, 113105 (2006).
- [12] H. Wu *Phys. Rev. B* **64**, 92413 (2001).

- [13] E. Zhitlukhina, K. Lamonova, S. Orel, P. Lemmens and Y. Pashkevich, J. Phys. Condens. Matter **19**, 156216 (2007).
- [14] S.Pandey, Ashwani Kumar, S. Patil, V. R. R. Medicherla, R. Singh, K. Maiti, D. Prabhakaran, A. Boothroyd, and A. V. Pimpale, Phys. Rev. B **77**, 045123 (2008).
- [15] Z. Y. Wu, M. Benfatto, M. Pedio, R. Cimino, S. Mobilio, S. R. Barman, K. Maiti and D. D. Sarma, Phys. Rev. B **56**, 2228 (1997).
- [16] S. Berman and D. Sharma, Phys. Rev. B **49**, 13979 (1994).
- [17] S. Pandey, S. Patil, V. Medicherla, R. Singh, and K. Maiti, Phys. Rev. B **77**, 115137 (2008).
- [18] C. Frontera, J. García-Muñoz, A. Llobet, M. Aradhana, J. Carvajal, M. Respaud, J. Broto, B. Raquet, H. Rakoto and M. Goiran, J. Alloys Compd. **323-324**, 468 (2001).
- [19] S. Roy, M. Khan, Y. Guo, J. Craig and N. Ali, Phys. Rev. B **65**, 064437 (2002).
- [20] W. Kim, E. Chi, H. Choi, N. Hur, S. Oh, and C. Ri, Solid State Commun, **116**, 609 (2000).
- [21] J. Burley, J.F. Mitchell, S. Short, D. Millar and Y. Tang, J. Solid State Chem., **170**, 339 (2003).
- [22] V. Plakhty , P. Chernenkov, S. Barilo, E Podlesnyak , E. Pomjakushina, E. Moskvina and S. Gavrilov, Phys. Rev. B **71** 214407 (2005).
- [23] F. Fauth, E. Suard, V. Caignaert and I. Mirebeau, Phys. Rev. B **66** 184421 (2002).
- [24] M Soda, Y. Yasui, M. Ito, S. Iikubo and M. Sato, J. Phys. Sco. Jpn. **72**, 1729 (2003).
- [25] C. Frontera, J. Luis Garcia-Munoz, A. Carrillo, Miguel A. G. Aranda, I. Margiolaki and A. Caneiro Phys. Rev. B **74**, 054406 (2006).
- [26] A .Taskin , Lavrov A. N. and Ando Phys. Rev. Lett. **90** 227201 (2003).
- [27] H. Luetkens, M. Stingaciu, Y. Pashkevich, K. Conder, E. Pomjakushina, A. Gusev, K. Lamonova, P. Lemmens and H. Klauss, Phys. Rev. Lett. **101** 017601 (2008).
- [28] H. Wu J. Phys.: Condens. Matter **15** 503 (2003).
- [29] W. Flavell, A. Thomas, D. Tsoutsou, A. Mallick, M. North, E. Seddon, C. Cacho, A. Malins, S. Patel, R. Stockbauer, R. Kurtz, P. Sprunger, S. Barilo, S. Shiryaev, and G. Bychkov Phys. Rev. B **70**, 224427 (2004).
- [30] Z. Zhou, S. McCall, C. Alexander, J. Crow, and P. Schlottmann, Phys. Rev. B **70**, 024425 (2004).

- [31] L. Sudheendra, Md. Motin Seikh, A. R. Raju, Chandrabhas Narayana Chem. Phy Letters **340** 275-281 (2001).
- [32] N. Kasper , I. Troyanchuk , D. Khalyavin , N. Hamad , L. Haupt, P. Froebel, K. Baerner, E. Gmelin, Q. Huang, and J.W. Lynn, Phys. Stat. Sol. (b) **215**, 697 (1999).
- [33] M. Imada, A. Fujimori, and Y. Tokura, Rev. Mod. Phys. **70**, 1039 (1998).
- [34] I. Nekrasov, S. Streltsov, M. Korotin, and V. Anisimov, Phys. Rev. B: Condens. Matter **68**,235113 (2003).
- [35] R. Mortimer, J. Powell and N. Vasanthacharya Sybth. Met. **71**, 2045 (1995).
- [36] S. Tajima, A. Masaki, S. Uchida, T. Matsuura, K. Fueki and S. Sugai J. Phys. C **20**, 3469 (1987).

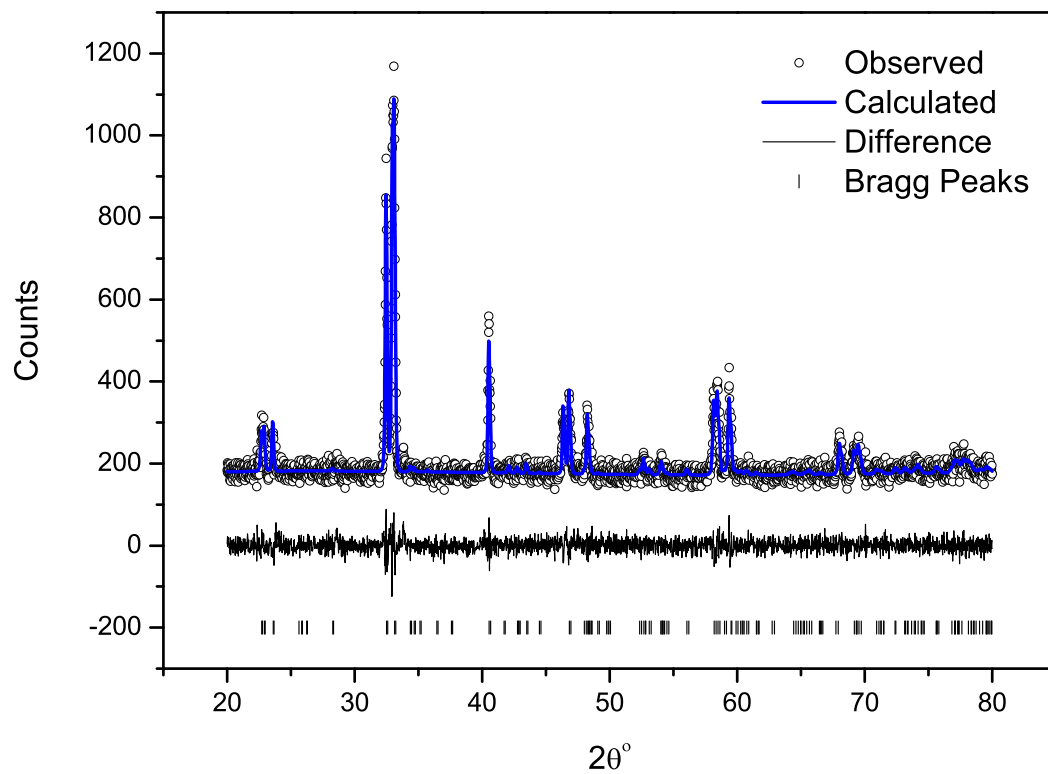


Fig. 1. Rietveld fitted XRD pattern of  $\text{GdBaCo}_2\text{O}_{5.5}$ . Circles represent experimental data, continuous line through the data is the fitted curve and the difference pattern is shown at the bottom as solid line.

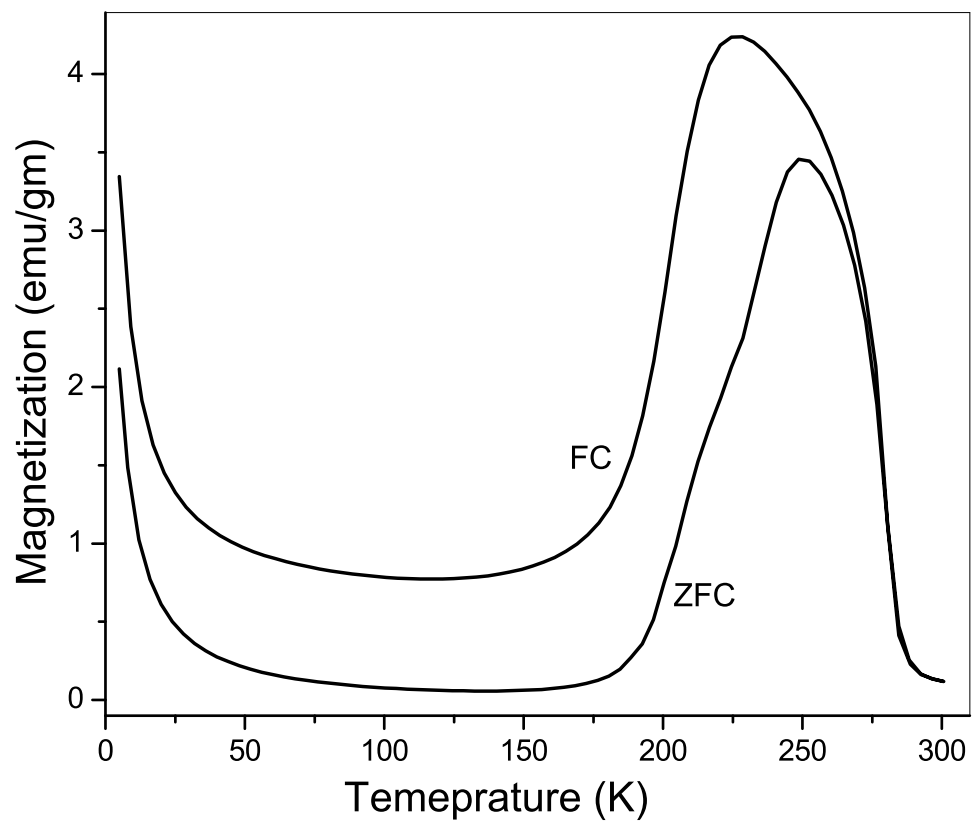


Fig. 2. Plot of magnetization versus temperature for GdBaCo<sub>2</sub>O<sub>5.5</sub>.

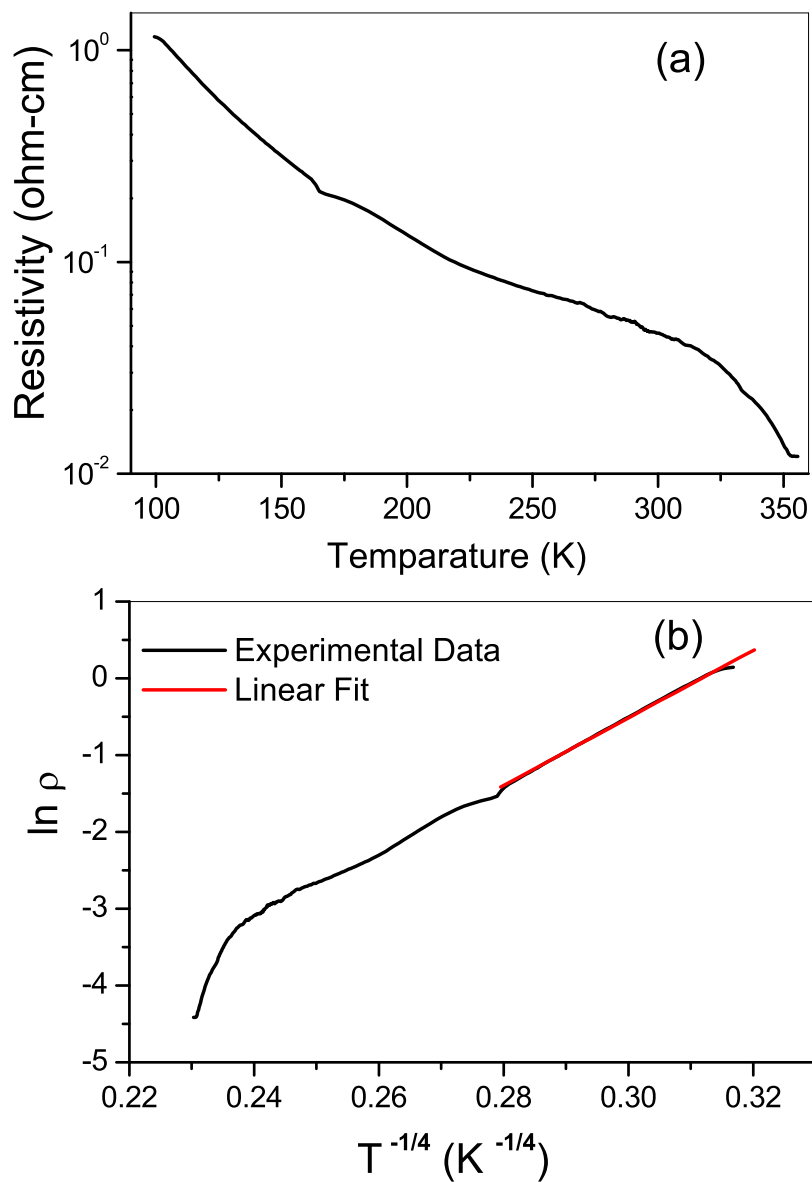


Fig. 3. (a) Plot of resistivity as a function temperature for GdBaCo<sub>2</sub>O<sub>5.5</sub> (b) Resistivity versus  $T^{-1/4}$  data for GdBaCo<sub>2</sub>O<sub>5.5</sub> fitting to VRH model.

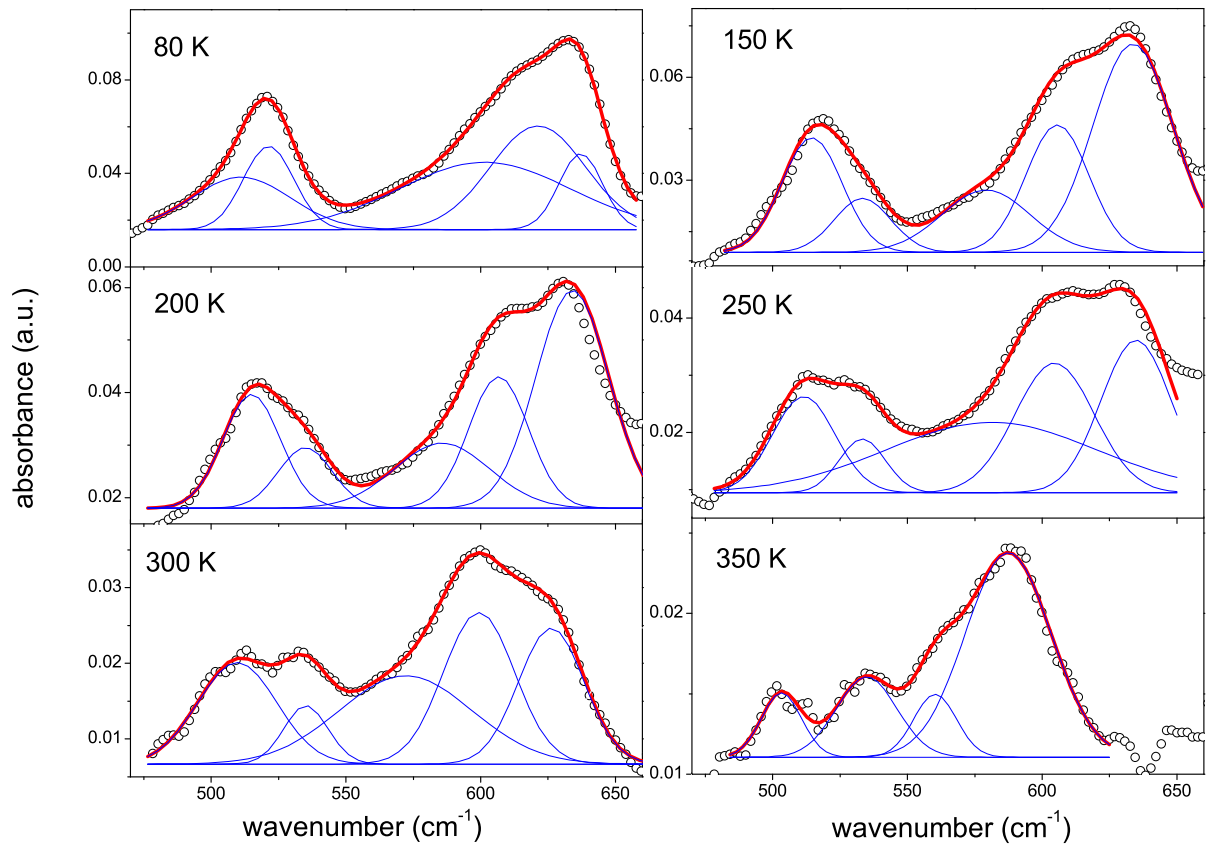


Fig. 4. IR absorption spectra recorded at various temperatures for  $\text{GdBaCo}_2\text{O}_{5.5}$  along with best fitted curves (solid line) which is a sum of four or five constituent Gaussian peaks.

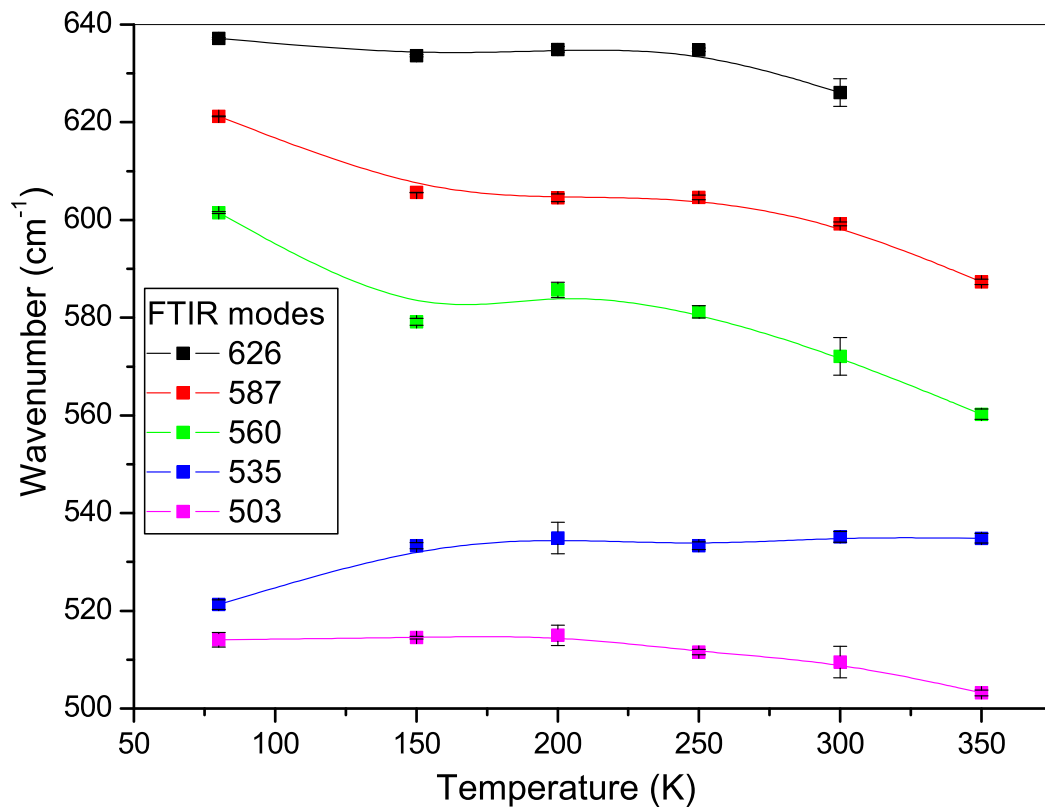


Fig. 5. Evolution of IR stretching modes with temperature for GdBaCo<sub>2</sub>O<sub>5.5</sub>.